CHIN. PHYS. LETT. Vol. 28, No. 11 (2011) 117803

Structural and Optoelectronic Properties of Cubic $CsPbF_3$ for Novel Applications

G. Murtaza[1], Iftikhar Ahmad[1,2**], M. Maqbool[3], H. A. Rahnamaye Aliabad[4], A. Afaq[5]

[1]*Materials Modeling Laboratory, Department of Physics, Hazara University, Mansehra, Pakistan*
[2]*Department of Physics, University of Malakand, Chakdara, Pakistan*
[3]*Department of Physics and Astronomy, Ball State University, Indiana, USA*
[4]*Department of Physics, Sabzevar Tarbiat Moallem University, Sabzevar, Iran*
[5]*Center of Excellence in Solid State Physics, Qua-e-Azam Campus, Lahore, Pakistan*

(Received 28 May 2011)

Chemical bonding as well as structural, electronic and optical properties of $CsPbF_3$ are calculated using the highly accurate full potential linearized augmented plane-wave method within the framework of density functional theory (DFT). The calculated lattice constant is found to be in good agreement with the experimental results. The electron density plots reveal strong ionic bonding in Cs-F and strong covalent bonding in Pb-F. The calculations show that the material is a direct and wide bandgap semiconductor with a fundamental gap at the R-symmetry point. Optical properties such as the real and imaginary parts of the dielectric function, refractive index, extinction coefficient, reflectivity, optical conductivity and absorption coefficient are also calculated. Based on the calculated wide and direct bandgap, as well as other optical properties of the compound, it is predicted that $CsPbF_3$ is suitable for optoelectronic devices and anti-reflecting coatings.

PACS: 78.20.−e DOI: 10.1088/0256-307X/28/11/117803

Perovskites have gained high technological and fundamental importance due to their commonly observed features such as high thermoelectric power, ferroelectricity, superconductivity, charge ordering, spin dependent transport, colossal magneto-resistance, and the interplay of structural, magnetic and optical properties.[1,2] These materials are frequently used as sensors, substrates, catalytic electrodes in fuel cells and are also promising candidates for optoelectronics.[3]

Metal fluorides have unique optical properties such as low refractive index and are extensively used as antireflection and protective coatings. It is well known that they can exhibit fast ion conduction. Fast fluoride ion conduction has been observed in $CsPbF_3$.[4−6] The relatively simple crystal structure, chemical bonding, and high fluorine diffusivity in a wide temperature range makes the single crystal of $CsPbF_3$ a convenient model for the investigations of the ionic diffusion.[5] A preliminary measurement of the diffraction pattern at ambient temperature confirms that $CsPbF_3$ is a cubic perovskite ($Pm3m$).[7]

Though $CsPbF_3$ has mostly been studied experimentally, however no theoretical studies are reported on it, except its structural and thermodynamic properties which are investigated by the MP2(full) and B3LYP hybrid functionals.[8] As $CsPbF_3$ is a direct bandgap compound and hence is optically active, it can be effectively used in photonic and optoelectronic devices. Though it is a potential compound for optical devices working in the high frequency range, even then no experimental or theoretical data is available about its optoelectronic properties.

In this Letter, we investigate the chemical bonding as well as structural, electronic and optical properties of cubic $CsPbF_3$ using density functional theory (DFT). This work will help to understand the structural and optoelectronic nature of the compound and will predict its technological importance. This study will also cover the lack of theoretical data on cesium lead-fluoride perovskite.

In the present calculations we have used the full potential linearized augmented plane-wave (FP-LAPW) method within the Wu-Cohen generalized gradient approximation (GGA),[9] as implemented in the wien2k code,[10] to solve the Kohn-Sham equations[11] for $CsPbF_3$. In the full potential scheme the unit cell of the crystal is partitioned into two different regions: (1) atomic spheres, (2) interstitial region (outside the atomic spheres). The wave function is expanded into two different basis sets. Within each atomic sphere the wave function is expanded in atomic-like functions (radial functions times spherical harmonics) while in the interstitial region it is expanded in a plane-wave basis. Inside the sphere the maximum value of l for the wave function expansion is $l_{\max}$=12. In the same manner the potential is expanded as

$$V(r) = \begin{cases} \sum\limits_{l,m} V_{lm}(r)Y_{lm}(r), & 1(a) \\ \sum\limits_{k} V_K e^{ikr}, & 1(b) \end{cases}$$

Equations 1(a) and 1(b) are for inside and outside the atomic sphere. The $R_{\rm MT}$ value of 2.5 a.u. is used for Cs, Pb and F atoms. For the wave function in the interstitial region the plane wave cut-off value of $K_{\max} = 9/R_{\rm MT}$ is chosen. For the k-space integra-

*Corresponding author. Email: ahma5532@gmail.com

tion in the irreducible Brillouin zone (IBZ); modified tetrahedron method[12] with 35 k-points is used to obtain self-consistency. The calculations of the optoelectronic properties are carried out by using a denser mesh of 2300 k-points in the IBZ.

Table 1. The calculated lattice constant a(Å), bulk modulus B(GPa), pressure derivative of bulk modulus B', and total ground state energy $E_0(Ry)$, of $CsPbF_3$ compared with the other theoretical and experimental results.

	This Work	Experimental results	Other calculations
V_0 (Å^3)	109.041	108.864[7]	
a(Å)	4.777	4.774[7]	4.795[14] 4.653[15]
B (Mbar)	0.52		
B'	5.11		
E_0 (Ry)	−60201.5279		
E_g^{R-R} (eV)	3.8		
E_g^{M-M} (eV)	5.7		
E_g^{X-X} (eV)	5.9		

The unit cell volume of $CsPbF_3$ is optimized to evaluate the structural parameters of the compound such as the lattice constant a, bulk modulus B, and pressure derivative of bulk modulus, B'. In the volume optimization process, the unit cell volume is varied and for each volume the corresponding total energy of the cell is calculated. The volume versus energy is fitted by the Birch–Murangan equation of state,[13] as shown in Fig. 1. The volume corresponding to the minimum energy in the plot is known as the ground state volume (V_0). At the ground state, a(Å), B(GPa) and B' are evaluated. The comparison of these optimized parameters, including the ground state energy, with the experimental and other calculated results are presented in Table 1. Our calculated optimized volume and lattice constant are in good agreement with the experiments and are better than the other theoretical results.[14,15]

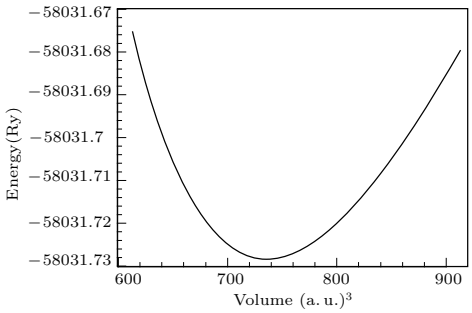

Fig. 1. Total energy as a function of unit cell volume for $CsPbF_3$.

In electronic properties, band structure and density of states for $CsPbF_3$ are calculated and shown in Figs. 2 and 3. From Fig. 2, it is clear that the minimum of conduction band (CB) and the maximum of valence band (VB) are at the R-symmetry point. Hence cesium leadfluoride in cubic phase is a direct band gap compound. The direct band gaps at other symmetry points (M, X) are also evaluated. The calculated band gaps at different symmetry points are presented in Table 1. Unfortunately, there is no theoretical or experimental data reported on the bandgap of $CsPbF_3$ with which we can compare our results, but due to the use of high k-point mesh in the IBZ and the Wu-Cohen GGA we are confident about the accuracy of our calculated bandgaps. This study can be used as a reference work for further theoretical and experimental studies on the bandgap nature of the compound.

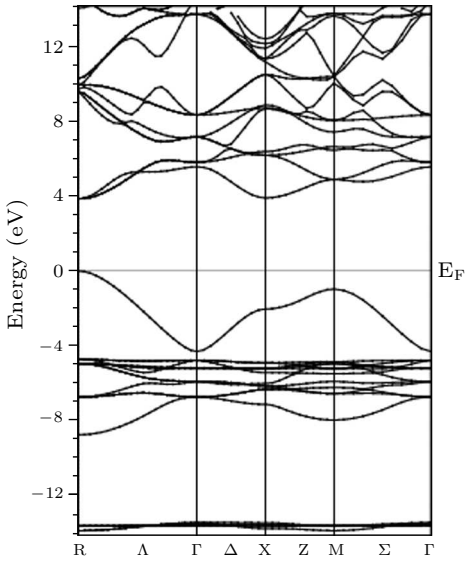

Fig. 2. The electronic energy band structure for $CsPbF_3$.

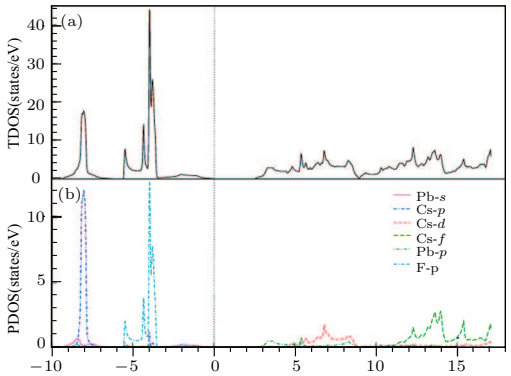

Fig. 3. Total density of states (a) and partial density of states (b) for $CsPbF_3$.

The density of states helps us to understand the electronic bandgap nature of a compound. In Fig. 3, the total and partial densities of states of $CsPbF_3$ are presented. On the basis of different bands; the total density of states (TDOS) could be grouped into three regions and the contribution of different states in these bands can be seen from the partial density of states (PDOS). The first region around −8.0 eV comprises a narrow band due to the Cs $5p$ state clearly from PDOS. The second region near the Fermi level within the range −6.0–0 comprises the VB. In this band the major contribution comes from the F $2p$ state. The third region after the Fermi level is the CB. The lower part of this band near the Fermi level is mainly due

to the Pb $6p$ and Cs $4d$ states, while the upper part of this band is due to the contribution from the Cs $4f$ state.

In order to foresee the chemical bonding and charge transfer in $CsPbF_3$, charge-density behaviors in 2D and 3D are calculated in the (110) plane and are shown in Figs. 4(a) and 4(b), respectively. From the figures it is clear that there is no electron accumulation (charge contours are completely closed) between Cs and F as well as a very low electron population at the Cs sites. This shows strong ionic bonding nature in the Cs-F bond. It can also be seen that most of the charge is populated in the Pb-F bond direction, while the maximum charge resides on the Pb and F sites. Due to small electronegativity difference of Pb (2.33) and F (3.98) as compared to Pb and Cs (0.79), less transfer of charge occurs in PbF_2 as compared to CsF. While charge is being shared in the PbF_2 bond which indicates strong covalent nature. The covalent behavior is due to the hybridization of Pb s and Pb p with the F p states of the valence band near the Fermi level. However the covalent bonding is not very strong as low charge resides between the Pb and F contours, which is clear from Fig. 4(b), while the maximum charge on the Pb and F sites. Hence, $CsPbF_3$ has a strong ionic bonding in CsF and partial ionic and covalent behavior in PbF_2. Similar bonding character is also reported in the isoelelectronic compounds $CsPbM_3$(Cl,Br,I)[16] to $CsPbF_3$.

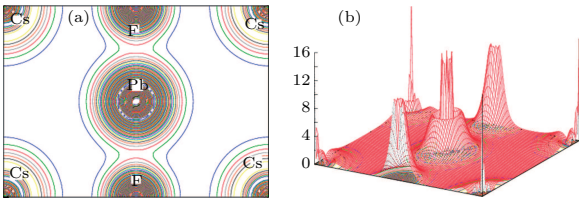

Fig. 4. Electron density for $CsPbF_3$ along (110) plane in 2D (a) and in 3D (b).

The knowledge of the optical properties of a material is extremely important for its possible applications in optoelectronic devices. Optical properties of $CeBO_3$, CeB_3O_6[17] and $CaTiO_3$[18] are calculated and found in excellent agreement with the experimental results. In the present work we apply the same theory to calculate the optical properties of $CsPbF_3$. Complex dielectric $\varepsilon(\omega) = \varepsilon_1(\omega) + \mathrm{i}\varepsilon_2(\omega)$ is an important optical parameter which describes the complete response of any material to the applied electromagnetic photons. The imaginary part $\varepsilon_2(\omega)$ is directly related to the electronic band structure of a material and describes the absorptive behavior. Following Khan *et al.*,[19] the frequency-dependent $\varepsilon_2(\omega)$ for crystals with cubic symmetry is given by

$$\varepsilon_2(\omega) = \frac{8}{2\pi\omega^2} \sum_{n,n'} \int_{BZ} |P_{nn'}(k)|^2 \frac{dS_k}{\nabla\omega_{nn'}(k)}, \qquad (2)$$

where $|P_{nn'}(k)|$ is the dipole matrix element between the initial and final states, S_k is an energy surface with a constant value, and $\omega_{nn'}(k)$ is energy difference between the two states.

The real part $\varepsilon_1(\omega)$ is obtained by using the Kramers–Kronig relation[20]

$$\varepsilon_1(\omega) = 1 + \frac{2}{\pi} P \int_0^\infty \frac{\omega' \varepsilon_2(\omega')}{\omega'^2 - \omega^2} d\omega'. \qquad (3)$$

Next, we evaluate other important optical parameters such as refractive index $n(\omega)$, extinction coefficient $k(\omega)$, reflectivity $R(\omega)$, energy loss function $L(\omega)$, optical conductivity $\sigma(\omega)$, and absorption coefficient $\alpha(\omega)$, in terms of real and imaginary parts of dielectric function.[3] These parameters are depicted in Fig. 5.

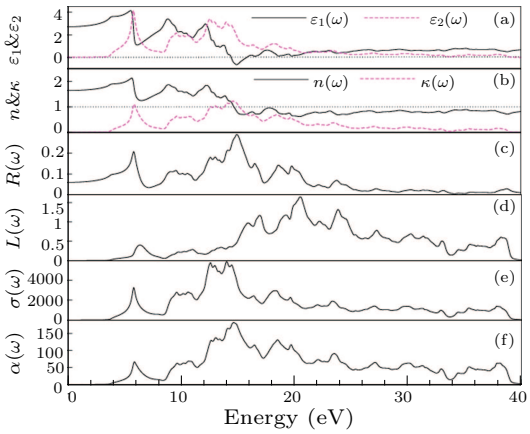

Fig. 5. Real and Imaginary parts of dielectric function (a), refractive index and extinction coefficient (b), reflectivity (c), energy loss function (d), optical conductivity (e), and absorption coefficient (f) versus energy.

For the compound under study, the dielectric function is calculated as a function of incident photon energy in the range 0–40 eV. In Fig. 5(a), $\varepsilon_2(\omega)$ is shown. We can see that the threshold point (onset) in the spectra of $\varepsilon_2(\omega)$ is found at 3.76 eV, which is due to the transition of electrons from mixed Pb $6s$ and F $2p$ states in the VB to the Pb $6p$ states in the CB near the Fermi level as clearly seen from Fig. 3(b). This point is closely related to the fundamental bandgap of the compound, 3.8 eV. Different characteristic peaks beyond the critical points can also be identified from the density of states (Fig. 3(b)). The peaks around 5.86 eV and 9.65 eV originates from the electronic transitions from F $2p$ and Pb $6s$ in the VB to the Pb $6p$ state in the conduction band. The peaks around 12.61 eV and 14.14 eV are formed by the electronic transitions from F $2p$, Pb $6s$ and Cs $5p$ states of VB to Cs $4d$ and Pb $6p$ states in the CB. The last noticeable peak around 18.19 eV is due to the transition from the F $2p$ state in the VB to the Cs $4f$ state in the CB.

Frequency-dependent $\varepsilon_1(\omega)$ is also shown in Fig. 5(a). In the spectra the most important quantity is the zero frequency limit $\varepsilon_1(0)$, which is the electronic part of the static dielectric constant. Our calculated $\varepsilon_1(0)$ for $CsPbF_3$ is 2.707. From its zero-frequency limit, it starts increasing and reaches the

maximum value of 4.130 at 5.62 eV, and then it decreases with noticeable variations. Also it goes below zero in the range 14.49–15.82 eV. In this range the incident photon beam is completely attenuated. As materials behave metallic for negative values of $\varepsilon_1(\omega)$ and are dielectric otherwise,[3] in this ranges of energy, $CsPbF_3$ is metallic.

Refractive index and extinction coefficient are plotted in Fig. 5(b). Interestingly $k(\omega)$ has the same trend as of $\varepsilon_2(\omega)$. It is further seen from the spectrum of $k(\omega)$ that the maximum absorption in the medium occurs at 14.14 eV.

The calculated refractive index for the compound is 1.645. It is clear from the figure that the refractive index of the material increases from its zero-frequency limit and reaches the maximum value of 2.134 at 5.7 eV. Beyond the maximum value it starts decreasing and goes below unity after 14.73 eV. Refractive index less than unity ($V_g = c/n$) shows that the group velocity of the incident radiation is greater than c.[21,22] This means that the group velocity shifts to negative domain and the nature of medium changes from linear to nonlinear. In other words, the material becomes superluminal for high energy photons.

Frequency-dependent reflectivity $R(\omega)$ for the compound is shown in Fig. 5(c). The zero-frequency reflectivity is 5.95%, which remains almost the same up to 4 eV. The small value of reflectivity in the infrared and visible energy range shows that the material is transparent in this range. Thus it can be used as an anti-reflecting coating in this part of the energy spectrum. After 4 eV it increases sharply and eventually becomes maximal (29%) at 14.98 eV with noticeable smaller peaks at other energies too. Interestingly, the maximum reflectivity occurs where the $\varepsilon_1(\omega)$ goes below zero, as seen from Figs. 5(a) and 5(c). The frequency corresponding to the plasma resonance can be calculated from the energy loss spectrum shown in Fig. 5(d). The resonant energy loss is seen at 20.53 eV, which corresponds to plasma frequency 2.7×10^{15} Hz.

Optical conductivity spectra $\sigma(\omega)$ is shown in Fig. 5(e). From the figure it is seen that the optical conduction starts around 3.8 eV. Then it increases and goes through smaller peaks, then rises to the maximum value of 5895.56 $\Omega^{-1}\text{cm}^{-1}$. Similar features are also observed for the absorption coefficient, $\alpha(\omega)$, (Fig. 5(d)) with the absorption range 5–39 eV. The wide absorption energy range predicts the usefulness of the compound for various optical and optoelectronic devices working in this range.

In summary, the FP-LAPW method within the Wu-Cohen GGA is applied to calculate chemical bonding as well as structural, electronic and optical properties of $CsPbF_3$. The lattice constant is found to be in good agreement with the experimental results. It is found that the compound has a wide and direct bandgap of 3.8 eV. The compound has strong ionic bonding (CsF) with weak covalent bonding (PbF_2) too. Different structures appear in the spectrum of the imaginary part of dielectric function, mainly due to the transitions from the Cs p and F p states in the VB to unoccupied states in the CB. The material becomes metallic in the range 14.49–15.82 eV while dielectric otherwise. The zero frequency reflectivity is 5.95% while the maximum reflectivity (29%) appears at 14.98 eV. The direct bandgap nature and high absorption power of the compound in the visible and ultraviolet energy range predict the usefulness in optical and optoelectronic devices in this range. The material can also be used for anti-reflection coatings.

References

[1] Moskvin S et al 2010 *Phys. Rev.* B **82** 035106
[2] Weeks C and Franz M 2010 *Phys. Rev.* B **82** 085310
[3] Murtaza G et al 2011 *Opt. Mater.* **33** 553
[4] Chadwick A V et al 1983 *Solid State Ionics* **9-10** 555
[5] Bouznik V M et al 1976 *Chem. Phys. Lett.* **37** 464
[6] Bouznik V M et al 1981 *Fast Ion Transport in Lead Fluoride with Perovskite-Like Structures, Defects in Insulating Crystals, Conference* (Rige USSR) p 499
[7] Berastegui P et al 2001 *J. Phys.: Condens. Matter* **13** 5077
[8] Boltalin A I at al 2007 *J. Phys. Chem.* A **111** 6534
[9] Wu Z and Cohen R E 2006 *Phys. Rev.* B **73** 235116
[10] Blaha P et al 2001 *WIEN2k, An Augmented plane-wave Plus Local Orbitals Program for Calculating Crystal Properties* (Vienna: Vienna University of Technology)
[11] Kohn W and Sham L J 1965 *Phys. Rev.* **140** A1133
[12] Erskine J L and Stern E A 1973 *Phys. Rev. Lett.* **30** 1329
[13] Birch F 1947 *Phys. Rev.* **71** 809
[14] Jiang L Q et al 2006 *J. Phys. Chem. Solids* **67** 1531
[15] Verma A S et al 2008 *Phys. Stat. Sol.* B **245** 1520
[16] Chang Y H and Park C H 2004 *J. Korean Phys. Soc.* **44** 889
[17] Dadsetani M and Pourghazi A 2006 *Phys. Rev.* B **73** 195102
[18] Yi L and Duan Y F 2005 *Chin. Phys. Lett.* **22** 435
[19] Khan M A et al 1993 *Phys. Rev.* B **23** 16974
[20] Wooten F 1972 *Optical Properties of Solids* (New York: Academic)
[21] Wang L J, Kuzmich A and Dogariu A 2000 *Nature* **406** 277
[22] Mugnai D, Ranfagni A and Ruggeri R 2000 *Phys. Rev. Lett.* **84** 4830